Microstructural and mechanical properties of low-carbon ultra-fine bainitic steel produced by multi-step austempering process

Mousalou, Hamid; Yazdani, Sasan; Avishan, Behzad; Ahmadi, Naghi Parvini; Chabok, Ali; Pei, Yutao

Published in:
Materials science and engineering a-Structural materials properties microstructure and processing

DOI:
10.1016/j.msea.2018.08.008

Publication date:
2018

Materials Science & Engineering A 734 (2018) 329–337

Contents lists available at ScienceDirect

Materials Science & Engineering A

journal homepage: www.elsevier.com/locate/msea

Microstructural and mechanical properties of low-carbon ultra-fine bainitic steel produced by multi-step austempering process

Hamid Mousalou[a], Sasan Yazdani[a,*], Behzad Avishan[b], Naghi Parvini Ahmadi[a], Ali Chabok[c], Yutao Pei[c]

[a] Faculty of Materials Engineering, Sahand University of Technology, Tabriz, Iran
[b] Department of Materials Engineering, Azarbaijan Shahid Madani University, Tabriz, Iran
[c] Department of Advanced Production Engineering, Faculty of Science and Engineering, University of Groningen, Nijenborgh 4, 9747 AG Groningen, the Netherlands

ARTICLE INFO

Keywords:
Bainite
Multi-step austempering
Mechanical properties
EBSD
SEM
XRD

ABSTRACT

The multi-step isothermal austempering heat treatment to achieve an ultra-fine bainitic microstructure and maximum volume fraction of bainite was conducted on a steel containing 0.26 wt% carbon. The microstructural and crystallographic characteristics, as well as the mechanical properties and fracture behavior were studied. The results showed that the subsequent austempering heat treatment at a lower temperature, immediately after partial bainite formation at a higher temperature, would replace the coarse austenite/martensite areas with much refined bainite consisting nanoscale plates of bainitic ferrite and filmy austenite which ultimately leads to the refinement of the bainitic microstructure. This microstructural modification, in addition to the increased yield strength, causes a significant increase in the impact fracture toughness of the multi-step austempered steels. The EBSD analysis also showed that the subsequent austempering heat treatment at a lower temperature results in a finer structure of Bain groups and increase in the fraction of high angle grain boundaries leading to higher resistance against crack propagation and subsequently higher impact energy absorption.

1. Introduction

Nanostructured Low-temperature Bainitic Steels (NLBS) have been the subject of extensive research due to their excellent mechanical properties. High strength and improved ductility have made them an excellent alternative material for producing many high-performance products. Their exceptional combination of high strength and ductility is directly related to the unique microstructural characteristics which can be obtained by isothermal bainitic transformation at low temperatures, i.e. 200–300 °C. The final microstructure consists of ultra-fine bainite including nanoscale bainitic ferrite plates and carbon enriched retained austenite [1–6]. Different parameters involved in exceptional strength properties of these materials among those, nanoscale microstructural features and high density of dislocations have the most significant role. Austenite presents in two filmy and blocky morphologies within the microstructure. Former has an almost identical thickness to that of bainitic ferrite subunits and micro blocks of retained austenites separate the bainitic sheaves. It has been shown that presence of significant amount of austenite films are mandatory to promote the ductility in these groups of high-performance steels [7–12]. Higher volume fractions of thinner bainitic ferrites would improve the mechanical properties to obtain higher yield strength and toughness [13]. Considering the necessity of very low transformation temperature to gain ultra-fine bainite, longer periods of time are required to finish the bainitic transformation and obtain the maximum volume fraction of bainitic ferrite. On the other hand, adding a significant amount of carbon (0.8–1 wt%) is necessary to reduce the bainite start (B_S) and martensite start (M_S) temperatures for conducting the isothermal bainite heat treatment at such low temperatures [1,14]. However, the high carbon content in the chemical composition restricts the weldability due to the potential for cracking in the heat-affected zone (HAZ) on flame cut edges and welds. Therefore, it is vital to reduce the amount of carbon as much as possible and simultaneously be able to attain the ultra-fine microstructural characteristics and consequently mechanical properties [15]. Previously, the partial replacement of carbon with some substitutional alloying elements such as Ni was proposed as an effective approach to simultaneously reduce the B_S and M_S temperatures, increase the hardenability and to keep the carbon at low concentrations. However, it has been shown that toughness of steel deteriorates with the formation of coalescence bainite [16,17]. Even, it has been shown that increasing the Ni content in low-carbon steels to higher than almost 5 wt%, would decrease the B_S below the M_S

* Correspondence to: P. O. Box: 51335/1996, Tabriz, Iran.
E-mail address: yazdani@sut.ac.ir (S. Yazdani).

https://doi.org/10.1016/j.msea.2018.08.008
Received 14 May 2018; Received in revised form 31 July 2018; Accepted 1 August 2018
Available online 05 August 2018
0921-5093/

temperature and consequently, bainite transformation would become impossible [15]. Accordingly, carbon addition into the chemical composition of the steel would be much effective than other alloying elements in decreasing both B_S and M_S temperatures and keeping the temperature gap enough for conducting the desired austempering heat treatment [14].

It seems possible to obtain the ultra-fine bainite in low carbon steels by designing a proper chemical composition and implementing a multi-step heat treatment. Although M_S temperature is not low enough in low carbon steels, partial ferrite formation within an intermediate temperature range, i.e. the ferrite-austenite region in the Fe-C phase diagram, would result in further carbon enrichment of remaining austenite and would reduce its M_S temperature sufficiently to be able to conduct the next step of isothermal bainitic heat treatment at lower temperatures. This method has already been used for obtaining TRIP steels even if the bainite transformation temperature was not that much low to obtain desired nanoscale bainite [18]. It is essential to use the proper amount of silicon and apply austempering heat treatment in different consecutive stages if further microstructural refinements are demanded in step austempering process. Silicon would retard the cementite precipitation when carbon partitioned from ferrite to surrounding austenite and carbon will remain in solid solution and will decrease the austenite M_S temperature. This would make it possible to conduct the bainite transformation in lower temperatures at next step of austempering. Since conducting the isothermal bainitic transformation in every other step further enriches austenite with carbon, it reduces the M_S temperature more and more making it possible to obtain finer bainite at lower temperatures. It would also become possible to replace austenite blocks with austenite films more efficiently [19,20].

In a previous research, Soliman et al. [21] showed that two-step austempering heat treatment resulted in considerably refined bainitic microstructure and consequently improved mechanical properties in alloyed low-carbon steel containing almost 0.26 wt% C. Similarly, Wang et al. [22] performed two and three-step austempering treatments on an alloyed medium carbon steel and they found that the mean thicknesses of bainitic plates formed in every next step of austempering treatment reduced and consequently improved tensile properties could be achieved compared to that of one-step conventional bainitic heat treatment. Two-step austempering treatment was also carried out in TRIP steels in order to reduce the second stage austempering temperature and it has been shown that it was more effective for improving the mechanical response of the materials in high-carbon TRIP steels rather than low-carbon steels [23]. Another study on a TRIP steel demonstrated that two-step austempering could change the morphology of the residual austenite from blocky to filmy type and could increase the mechanical stability of residual austenite during plastic deformation and thus better ultimate tensile strength and elongation combinations could be attained [24].

Although a proper chemical composition design and implementing a suitable heat treatment procedure are essential to gain ultra-fine bainite in low carbon steels, no clear and obvious relationships have been explained before between microstructural and crystallographic characteristics and mechanical response of those materials. This article aims to investigate the microstructural, crystallographic and mechanical properties evolutions in low carbon steels with ultra-fine bainitic microstructure obtained after single, two and three step austempering processes.

2. Materials and methods

Low-carbon steel with suitable chemical composition was designed using MUCG83™ thermodynamic model [25]. Attention paid to obtain low enough B_S and M_S temperatures as well as maintaining a proper difference between the two temperatures. Steel was melted in an induction furnace under an inert gas atmosphere and cast in a metallic cube mould with the cross-section of $4 \times 6\ cm^2$. Electroslag remelting (ESR) process was carried out using Al_2O_3-30% CaF_2 flux powder in order to obtain clean primary steel free from inclusions. The high solidification rate in ESR process could be also effective in minimizing the segregation degree of alloying elements [26]. Cast steel was homogenized at 1200 °C for 4 h and hot rolled at 900–1000 °C in several passes to reduce the thickness to about 15 mm. The final chemical composition of steel was Fe- 0.26C- 1.70Mn- 1.42Si- 1.10Cr- 1.10Ni- 0.94Cu- 0.24Mo- 0.10V all in weight percent.

Si was used to prevent the carbide precipitations and to increase the carbon activity during austempering heat treatment [27]. To control the grain size of the prior austenite and to prevent grain growth during the austenitization, 0.10 wt% vanadium was used. The other alloying elements were added to reduce the Bs and Ms temperatures, to increase the hardenability, to obtain a higher volume fraction of bainite (by shifting the T_0′curve to higher carbon concentrations) and to increase the primary austenite strength in steel. Appropriate heat treatment cycles were designed based on dilatometric tests being conducted on a Bahr Dil805A™ instrument using cylindrical specimens of 4 mm diameter and 10 mm in length. Dilatometric samples were machined from hot-rolled plate perpendicular to the rolling direction. Primarily the M_S, A_{C1} and A_{C3} temperatures of the raw material have been determined and consequently, kinetics of the bainite transformation and change in M_S temperature of retained austenite at every other stage of step-austempering processes have been evaluated.

For microstructural evaluations, the heat-treated samples were ground and mechanically polished followed by etching using 2% Nital etching solution. The microstructural studies were performed using Olympus PMG3™ optical microscope and Tescan MIRA3™ field emission gun scanning electron microscope. High-magnification SEM images were used to determine the thicknesses of ferrite plates and austenite films using the line intercept method [28]. To determine the volume fraction of residual austenite, X-ray diffraction analysis was implemented. For this aim, samples were etched and polished for several consecutive stages to obtain an undeformed surface and omit the effect of mechanical force during grinding stage. Then, the step-scanning was performed on samples using Brucker-D8 Advance™ Diffractometer with CuKα radiation at a voltage and current of 40 kV and 40 mA, respectively. Scanning was carried out in the 2θ range of 42–105° with a scan step of 0.01° and dwell time 1 s. The volume fraction of residual austenite was calculated using the integrated intensities of (200), (220) and (220) peaks of austenite and (200), (211) and (220) peaks of ferrite [29].

Hardness tests were carried out based on ASTM E92-82 standard test method using an HV30 scale and the average of at least 6 measurements from each sample was reported. For tensile tests, the flat samples were prepared with the gage lengths of 25 mm according to ASTM E8-09 standard method. Tensile samples were cut in the rolling direction and tensile tests were carried out using the Instron 8502™ tensile testing machine equipped with an extensometer at a strain rate of $3.3 \times 10^{-4}\ s^{-1}$. At least 3 tests were performed for each heat treatment condition to ensure the reproducibility. Charpy impact test samples were implemented according to ASTM E23-07 standard using $10 \times 10 \times 55$ mm notched samples. Notches were perpendicular to the rolling direction in all test samples and tests were carried out at room temperature using Roell Amsler™ impact testing machine. At least 4 samples were tested for each condition and the average values were reported in each case.

For orientation imaging microscopy (OIM), the heat treated steel samples were mechanically polished with 1 micrometer diamond spray and then electropolished in a 90% CH_3COOH +10% $HClO_4$ solution at 21 °C and 20 V voltage for 25 s. Finally, the OIM studies were carried out with electron backscatter diffraction pattern by a Philips ESEM-XL30™ scanning electron microscope equipped with a field emission gun operating at 20 kV using scan step size of 100 nm. The clean-up process of the raw OIM data were carried out by using neighbor confidence index correlation method on data points with confidence index

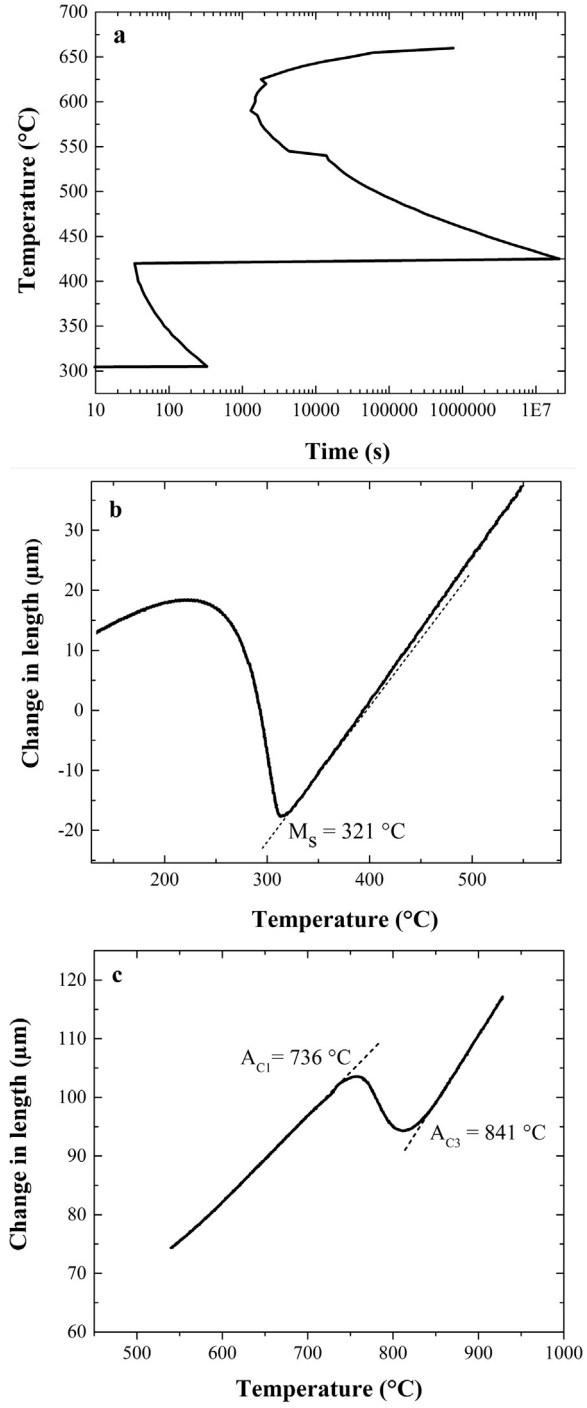

Fig. 1. (a) TTT diagrams obtained using MUCG83 thermodynamic model, (b) dilatometric curve to measure the M_S temperature and (c) dilatometric curve to measure the A_{C1} and A_{C3} temperatures.

lower than 0.1.

3. Results and discussion

Fig. 1a illustrates the time-temperature-transformation diagram (TTT) of the studied steel based on the MUCG83™ thermodynamic model according to which the M_S temperature was theoretically determined to be 302 °C. TTT diagram consisted of two upper and lower C curves predicting the kinetics of the reconstructive and shear transformations, respectively. Apart from those predictions by thermodynamic model, a suitable thermal cycle including heating up to 930 °C

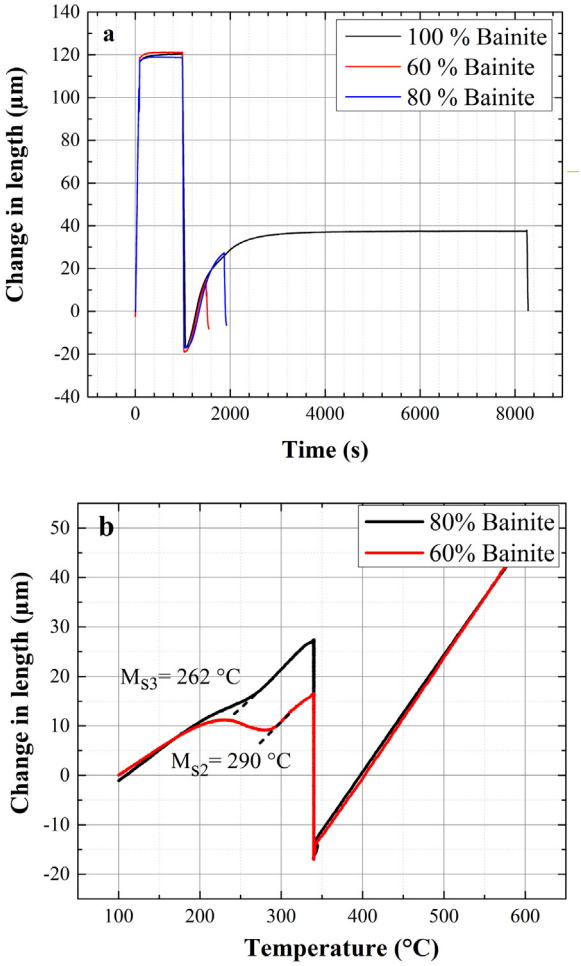

Fig. 2. (a) Dilatation curves showing the kinetics of bainitic transformation for obtaining 100%, 80% and 60% of the maximum bainite formed at 340 °C and (b) Dilatation curves to measure M_{S2} and M_{S3} temperatures.

with a rate of 5 °C s^{-1}, isothermally holding for 20 min and immediate cooling to the ambient temperature with a rate of 20 °C s^{-1} was carried out using dilatometer in order to obtain experimental critical temperatures to assist selecting a more precise heat treatment procedure. According to the experimental results depicted in Fig. 1b and c, the practical M_S temperature was 321 °C, and the A_{C1} and A_{C3} temperatures were determined to be 736 °C and 841 °C, respectively.

Dilatometric tests were also implemented to characterize the kinetics of bainite transformation in the steel. For this aim, the bainite heat treatment was carried out at 340 °C (20 °C higher than experimentally determined M_S of bulk material) and the changes in length were recorded with respect to the heat treatment until bainite transformation reached to its maximum content. As shown in Fig. 2, the results indicated that bainitic transformation terminated after almost 3000 s when the change in length of the specimen reached the plateau and no further change in length with time could be observed in dilatometry curve. Additionally, according to the results, about 480 s and 840 s were needed to attain 60% and 80% of the maximum bainite content within the microstructure at 340 °C, respectively. Dilatometric measurements were also carried out to determine the martensite start temperature of the remained untransformed austenite in steel when 60% and 80% of the maximum volume fraction of bainite formed within the microstructure, i.e. M_{S2} and M_{S3}, and results have been given in Fig. 2b. It can be seen that the M_{S2} and M_{S3} temperatures reduced to 290 and 262 °C, respectively, considerably lower than the M_S of the bulk steel. This could make it possible to perform the bainite

Table 1
Bainitic heat treatment cycles after austenitizing at 900 °C.

	Bainitic heat treatment cycles
Sample A	340 °C - 4 h
Sample B	340 °C - 8 min/305 °C - 6 h
Sample C	340 °C - 14 min/277 °C - 22 h
Sample D	340 °C - 14 min/277 °C - 22 h/200 - 54 h

transformation at lower temperatures in step austempering heat treatments.

According to the dilatometric results, four different heat treatment procedures were designed to achieve the desired low-temperature bainite as indicated in Table 1. A single-step austempering was performed on the first set of samples (A) as austenitizing at 900 °C and further austempering at 340 °C (20 °C above the practically determined M_S temperature) for 4 h to achieve full bainitic microstructure. Two-step austempering (B) was also designed in which samples were austenitized at 900 °C, partially transformed to bainite at 340 °C for 8 min to gain almost 60% bainite and finally quenched to 305 °C (15 °C above the practically determined M_{S2} temperature) and kept for 6 h. The third set of samples (C) austenitized at 900 °C, partially transformed to bainite at 340 °C for 14 min to attain 80% bainite, quenched to 277 °C (15 °C above the M_{S3}) and held for 22 h. The final set of samples (D) was a three-step austempering heat treatment in which samples were initially austenitized at 900 °C, partially transformed to bainite at 340 °C to gain 80% bainite, quenched to 277 °C (above the M_{S3}) and held for 22 h and finally quenched to 200 °C for 54 h. All heat treatments were carried out in salt bath furnaces and samples were quenched in water at the end of the designed heat treatment cycles to ambient temperature.

Further microstructural study was performed using scanning electron microscopy as shown in Fig. 3. It can be seen that the volume fraction and morphology of the austenite/martensite microblocks were different at the end of the different heat treatment cycles. The size of the blocks decreased significantly by performing two-step austempering (Fig. 3b and c) and reduced to a minimum by performing three-step austempering (Fig. 3d). Additionally, results indicated that the various heat treatment procedures ended in different thicknesses of bainitic ferrite and austenite plates. Fig. 3a shows the matrix of sample one step austempered at 340 °C consisting blocky shape austenites and bainitic ferrite plates of different thicknesses. The two-step austempering process has led to the formation of finer bainitic plates in the second stage (B_2) as indicated with arrows in Fig. 3b and c which the average plates size is less than the first stage (B_1) plates. Third generation of the bainitic plates (B_3) shown in Fig. 3d, observed in the microstructure after a three-step austempering treatment which further refined the microstructure and reduced the average thickness of the plates. Accordingly, multi-step austempering heat treatment refined the bainitic ferrites and austenite films to about 80 and 40 nm thicknesses while they were almost 140 and 70 nm thick by the single step austempering, respectively. Examples of nano-scale bainitic ferrites are shown in Fig. 3d. The results confirm that, by a proper multi-step austempering heat treatment, it is possible to achieve nano scale bainitic microstructure in low carbon steels. The austempering temperature and carbon concentration of decomposed austenite are the important parameters that affect the size of the microstructural features [30]. Lower transformation temperatures result in finer bainitic ferrites and austenite films and micro blocks due to the higher driving force of the bainitic transformation and higher strength of primary austenite. Stronger austenite more restricts the motion of glissile interface of ferrite/austenite and makes it possible to achieve finer subunits and austenite films. On the other hand, higher volume fractions of bainitic sheaves can be obtained at lower transformation temperatures which consume more primary austenite and decrease its average diameter. Considering the multi-step austempering in this study, conducting the bainite heat treatment at each lower transformation temperature at second and third stages resulted in

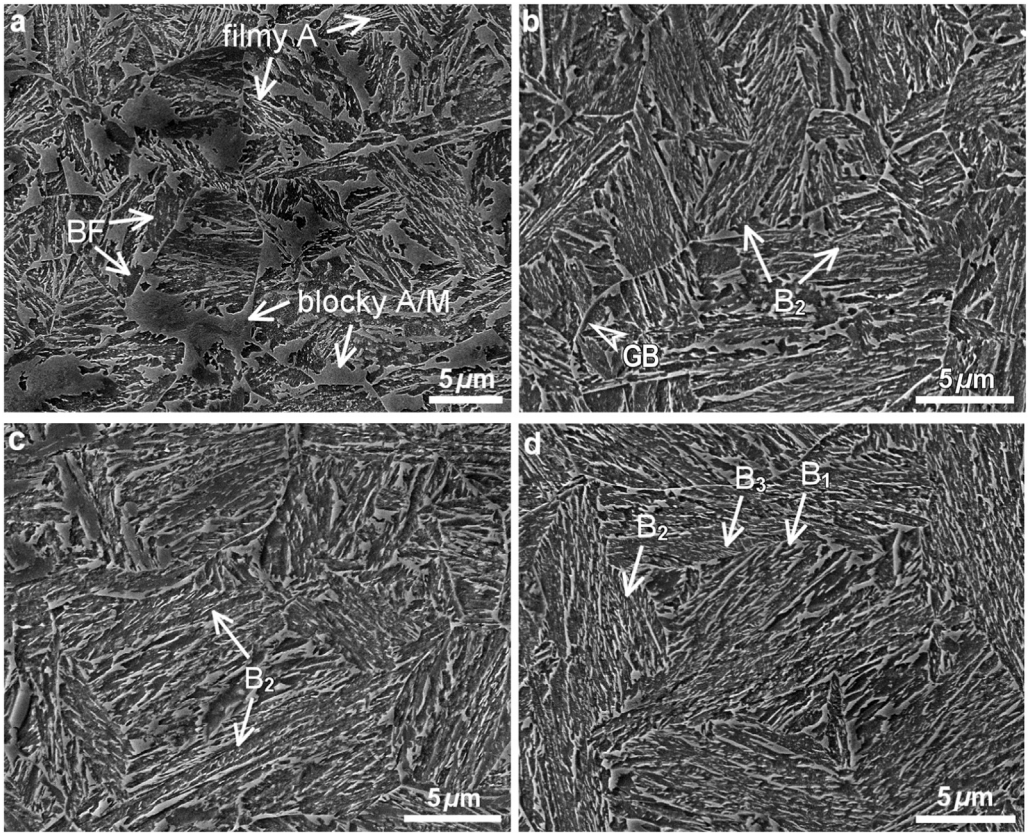

Fig. 3. SEM micrographs of (a) sample A, (b) sample B, (c) sample C and (d) sample D.

thinner bainitic ferrites and austenite and consequently decreased the average thickness of the microstructural features comparing to that of obtained by the ordinary single step austempering.

Formation of bainitic ferrite during the first and second austempering stages and carbon partitioning from bainitic ferrite to the surrounding austenite during the transformation increased the austenite carbon content at each heat treatment stage comparing to that of the previous one. As a result, the austenite that was decomposed to bainite in every other stage possessed higher carbon content and had lower M_S and B_S temperatures. The higher amount of carbon in solid solution in austenite further enhanced the austenite strength. Therefore, it was not a surprise to gain thinner microstructure by each second and third step of austempering comparing to that obtained by a single step heat treatment. Consequently, multi-step austempering made it possible to reduce the average thickness of bainitic ferrite and austenite and the more volume fraction of bainite formed at the second and third steps would further reduce the average size of the microstructure. Higher volume fractions of bainite formed at the second and third stages of heat treatment cycles and consequently more consumption of primary austenite explain the lower volume fraction of high carbon retained austenite and finer sizes of austenite/martensite blocks. According to the results, multi-step austempering treatment reduced the average size of A/M micro block from 2.8 μm in Sample A by the one-step austempering treatment to 0.83 μm after two-step austempering (Sample C), and 0.7 μm after the three-step process (Sample D).

Fig. 4 shows the variations of the volume fraction of residual austenite and hardness of the samples with respect to the heat treatment procedures. Quantitative values showed that using the two- and three-step austempering treatments reduced the volume fraction of residual austenite content and increased the hardness of the steels. This can be rationalized due to the further decomposition of parent austenite to bainite at lower transformation temperatures during the second and third stage of heat treatments. Additionally, since bainitic ferrites are harder than retained austenite, it is expected to gain higher hardness values. The highest amount of bainite in sample D resulted in the highest hardness value in this sample comparing to that of other test specimens.

Fig. 5 compares the engineering stress-engineering strain curves of the multi-step bainitic transformed steel samples, and the mechanical properties extracted from those curves are summarized in Table 2. The results indicate that the one-step austempering resulted in the highest elongation (15.1%) and considerable work hardening coefficient in comparison with the other samples. Nevertheless, multi-step austempering enhanced the yield strength of the steels from 880 MPa in Sample A to 1031, 1059 and 1061 MPa in samples B, C and D,

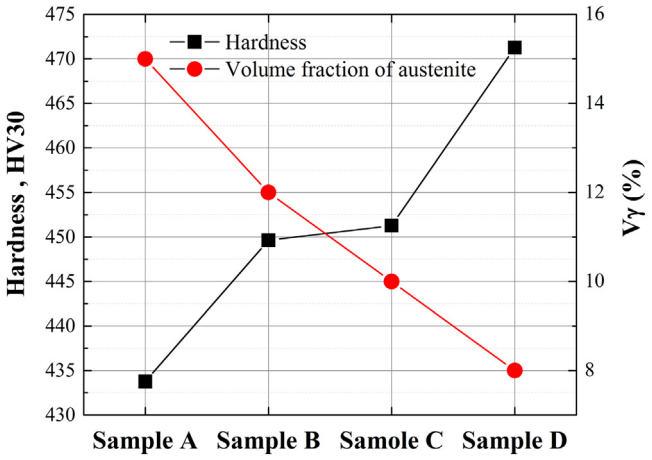

Fig. 4. Changes in the hardness and the volume fraction of retained austenite (V_γ) after different multi-step bainitic transformation.

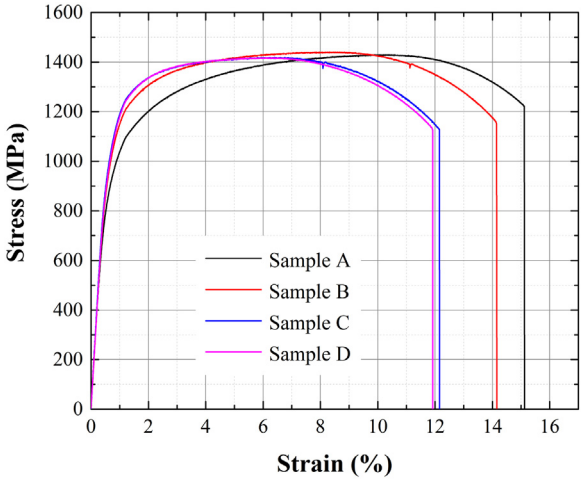

Fig. 5. Engineering stress–engineering strain curves of the heat treated steel samples.

Table 2
Mechanical properties of the heat treated steel samples.

Sample ID	YS (MPa)	UTS (MPa)	El (%)
Sample A	880	1428	15.1
Sample B	1031	1445	14.1
Sample C	1059	1422	12.1
Sample D	1061	1417	11.9

respectively, while there was no noticeable change in the ultimate tensile strength.

The variations of the mechanical properties are attributed to the microstructural evolutions by the different heat treatment procedures. High carbon retained austenite is the main contributing factor controlling the ductility, and higher volume fraction of retained austenite is necessary to obtain higher elongation. That is the reason for the higher measured elongation in sample A while it is lowered in samples B, C and D due to reduced austenite content. Care must be taken to the point that, besides the austenite content, its morphology and mechanical stability also affect the ductility of the steels in this study. The higher volume fraction of austenite films and consequently higher mechanical stability are mandatory to be able to reach a higher ductility. To summarize, austenite volume fraction, its morphology and its mechanical stability must be considered simultaneously during ductility assessments [23,31,32]. However, it seems that the higher volume fraction of austenite was the dominant factor in this study.

Similarly, microstructural constituents affect the strength properties. Bainitic ferrites are the main factors determining the strengths of the heat treated materials. Higher volume fractions of thinner bainitic subunits are mandatory for enhanced strength. The mean thicknesses of the bainitic ferrites were decreased by conducting the second and third step of austempering because the bainite formed at every other step was finer comparing to previous austempering step. The Hall-Patch equation and Langford-Cohen equation [13] are two general equations to express the relationship between grain size and strength. Once the slip distance is less than one micron, the second equation is more accurate. Accordingly, the reduced thickness in bainitic plates increased the strength of the steel in accordance with the above equations.

Fig. 6 shows the results of Charpy impact test at room temperature for all the heat treated samples. The results indicate that implementing the two or three step austempering process significantly enhances the impact energy of the materials comparing to that of ordinary single-step austempering heat treatment. This could be related to the microstructural variations and the change in austenite volume fraction and morphology. Although the volume fraction of retained austenite

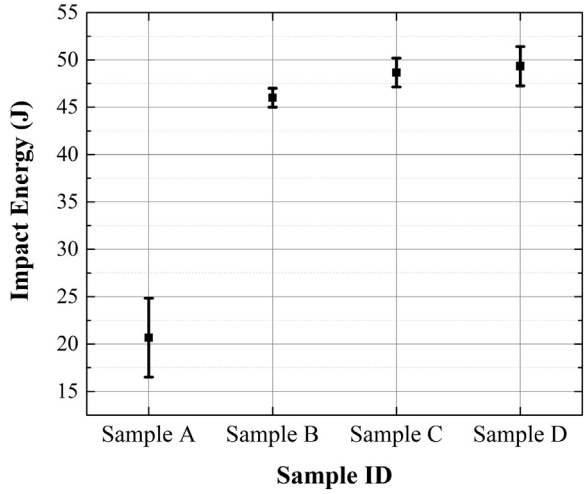

Fig. 6. Change in the impact energy of the heat treated steel samples.

reduced by applying the second stage and third stage of bainitic heat treatment, the higher volume fraction of austenite films among a lower fraction of austenite micro blocks and martensite strongly enhanced the impact toughness values. It has been shown that the volume fraction of the retained austenite is not the only factor affecting impact toughness values in carbide-free bainite and its morphology must also be considered simultaneously [33]. Austenite blocks are mechanically less stable and transform to martensite quickly and therefore cannot play the beneficial role in crack blunting and consequently toughness promotion. However, replacing austenite blocks with austenite films that are mechanically more stable can be helpful in toughness enhancement contrary to the lower volume fraction of austenite. Since the highest volume fraction of austenite films and more effective elimination of austenite blocks happened at the end of the three-step austempering heat treatments, it was logical to acquire the highest impact energy values. To summarize, the morphology of retained austenite, namely films instead of blocks, was more effective than its volume fraction when discussing the impact energy in this study. One cannot ignore the effect of bainitic ferrites on toughness properties. Higher volume fractions of finer bainitic ferrites formed at the end of two and three-step austempering heat treatments, which aligned in different crystallographic directions. As a result, finer bainitic sheaves in different directions were helpful in arresting and deflecting the cracks and consequently increasing the absorbed impact energy.

Fig. 7 compares the fracture surface of the samples formed by the Charpy impact test. It is evident that the multi-step austempered samples contain finer fracture dimples of larger area portion compared to that of the single-step heat treated materials, which approves a more ductile fracture mode. Besides, smaller fracture facets are those related to the smaller austenite micro-blocks present within the microstructure

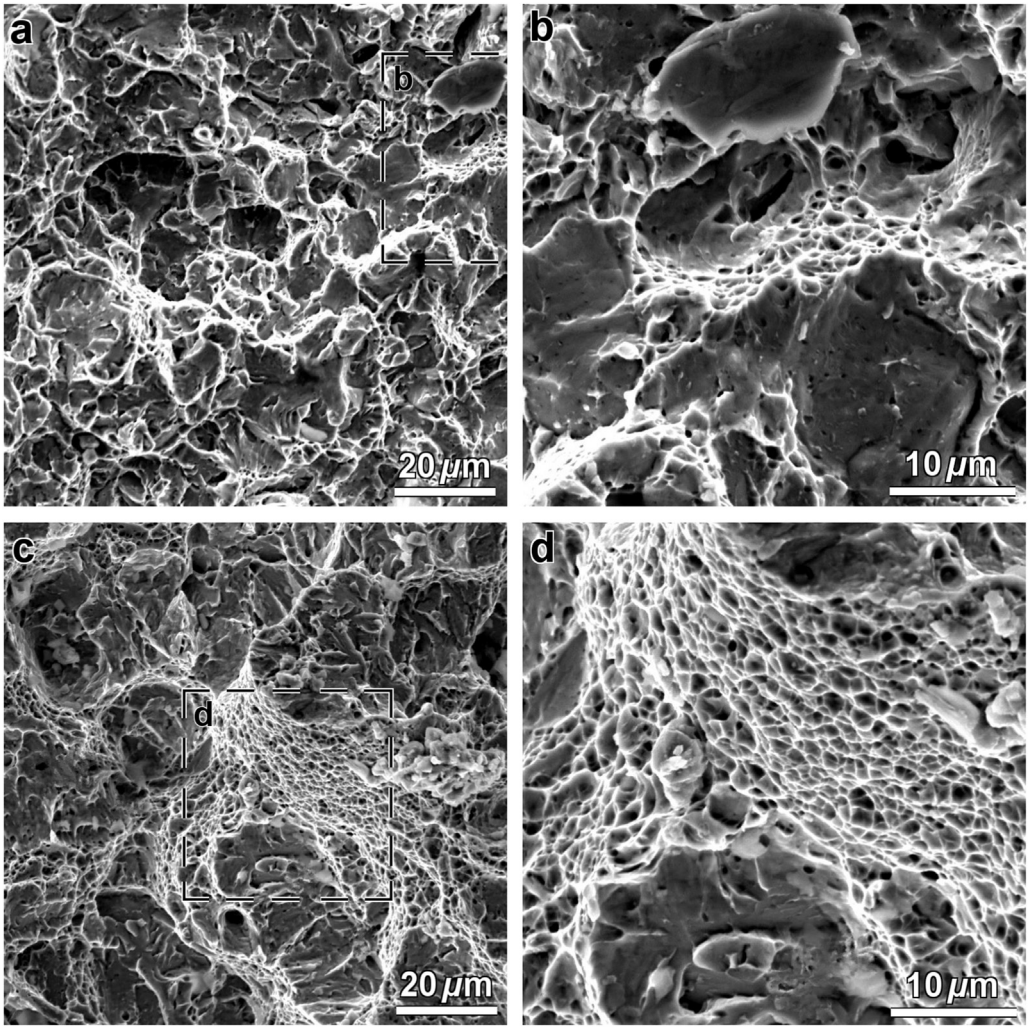

Fig. 7. Fracture surfaces of the heat treated steel samples after (a, b) single-step austempering (340 °C-4 h) and (c, d) two-step austempering (340 °C - 14 min/277 °C - 22 h) observed at different magnifications.

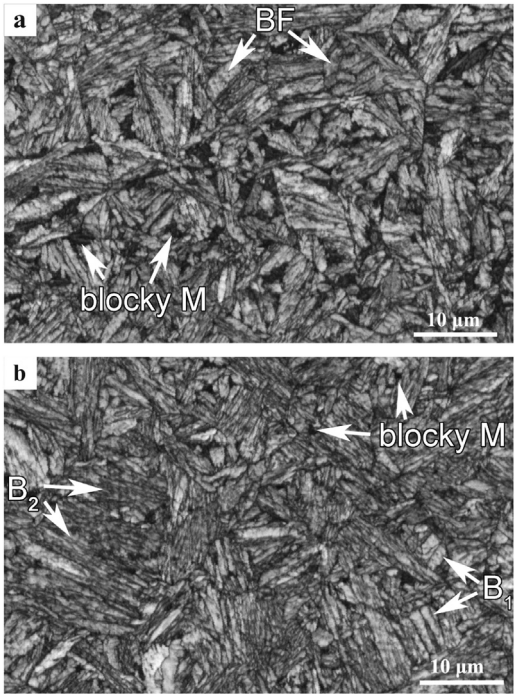

Fig. 8. EBSD image quality (IQ) maps of (a) single-step austempered (340 °C - 4 h) and (b) two-step austempered (340 °C - 14 min/277 °C - 22 h) steel samples.

of the multi-step austempered samples.

EBSD image quality (IQ) maps were acquired from the impact-fractured samples of one-step (Sample A) and two-step (Sample C) austempered steels and the results are shown in Fig. 8. Bainitic microstructure and martensitic islands (black areas) are quite obvious in the micrographs. The bainitic microstructure of the one-step austempered sample is coarser than that of the two-step austempered, and correspondingly larger and higher volume fraction of martensite microblocks are present within the microstructure. Formation of larger martensitic blocks in the fractured sample A can be directly related to the coarser austenite blocks remained at the end of the one-step austempering process at the isothermal temperature of 340 °C. Those larger austenite blocks were thermally and mechanically less stable and they transformed to martensite during cooling the material to the ambient temperature at the end of the treatment and also when samples were mechanically deformed during impact tests. In contrast, in sample C due to the higher driving force for bainite formation during the second step of heat treatment, the higher volume fraction of bainitic sheaves were formed which resulted in more consumption of primary austenite, and lower volume fractions and smaller austenite blocks were attained. Larger austenite blocks were replaced with bainitic ferrites and austenite films, the latter being mechanically and thermally more stable which had a positive effect on toughness enhancement as demonstrated before.

Fig. 9 shows the observed $\{011\}_\alpha$ and $\{001\}_\alpha$ pole figures of primary austenite grains and the calculated $\{011\}_\alpha$ and $\{001\}_\alpha$ pole figures based on K-S orientation relationship identified by overlaid black points in both pole figures. Comparing both calculated and experimental pole figures for the selected primary austenite grain approves that bainitic ferrites had K-S crystallographic orientation relationship with austenite. Three different colors in Fig. 9(a) and four different colors in Fig. 9(b) denoted Bain groups and Close-packed plane (CPP) groups, respectively. 24 variants based on the K-S orientation relationship were subdivided into four packets within one prior austenite grain based on K-S orientation relationship, and each packet consisted of 6 variants with the same habit plane in a single CPP group. In one packet based on the compression axis due to Bain strain, there are also

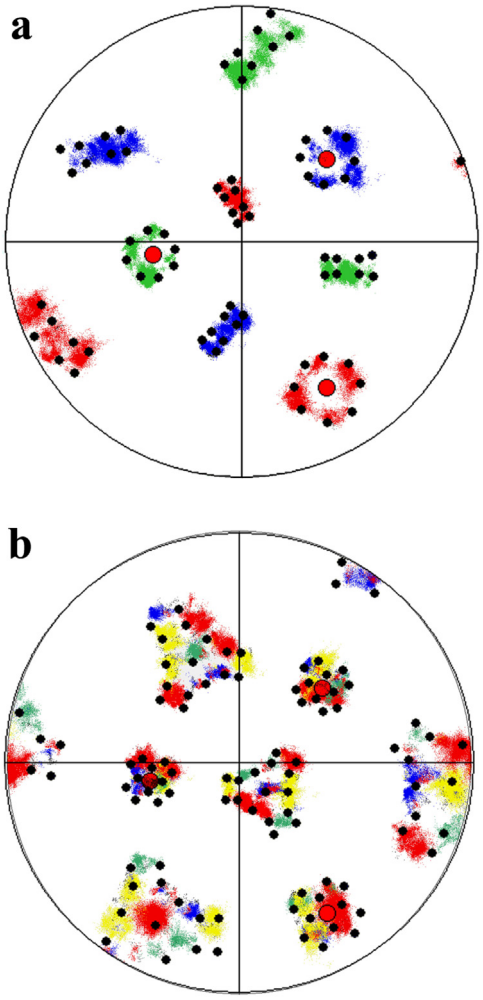

Fig. 9. (a) $\{001\}_\alpha$ and (b) $\{011\}_\alpha$ pole figures of the selected single primary austenite and overlaid standard pole figures (black dots) calculated assuming an ideal K-S orientation relationship.

three blocks or Bain groups composed of two variants belonging to the same Bain group. The complete information on the classification of 24 variants into packets and Bain groups as well as their orientation characteristics with respect to a reference variant (V1) has been given in previous studies [34,35].

The length fraction of high angle boundaries is another effective factor which must be taken into account when discussing the absorbed impact energy by the heat-treated samples, as high angle grain boundaries are strong barriers against the crack propagation that can arrest or deflect the crack path [36]. Bain groups map and packets map have been analyzed in order to study the nature of the boundaries more precisely as shown in Fig. 10 for sample A and sample C, respectively. Prior austenite grain boundaries have been highlighted by bold black lines. It is demonstrated that the boundary between variants belonging to one Bain group has a low angle misorientation (smaller than 21.1°) and is marked by white lines in the images while the boundary between the variants belonging to the different Bain groups exhibits a high misorientation angle (larger than 47.1°) that is marked by black lines in the images. According to Fig. 10, the major difference in crystallographic characteristics of the two samples is related to their Bain group map and there is not a significant difference in the packet map. The austempering treatment in the second steps at lower transformation temperatures in step austempering process leads to changes in the Bain group map compared to the conventional one-stage heat treatment. In other words, by lowering the austempering temperature in the second

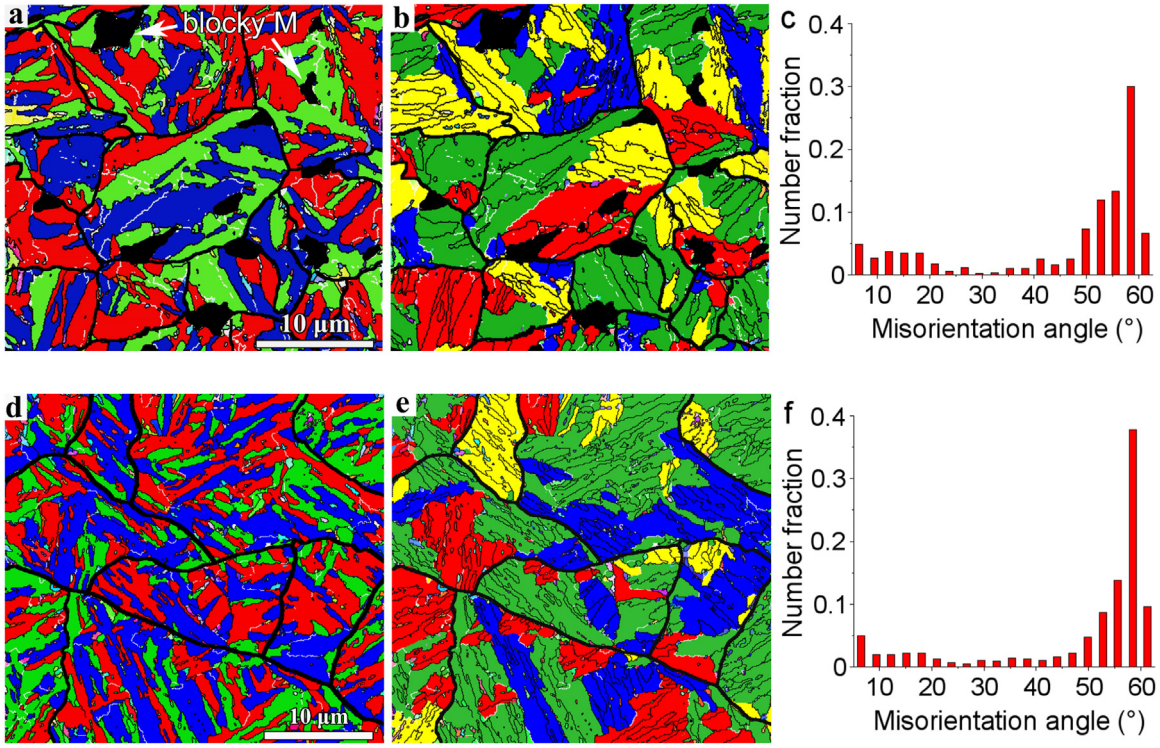

Fig. 10. Bain group map, the corresponding packet map and the fraction of boundaries with different misorientation angles of (a, b, c) the single-step austempering treated sample (340 °C - 4 h) and (d, e, f) the two-step austempering treated sample (340 °C - 14 min/277 °C - 22 h).

stage, the adjacent variants are more likely to be located in different Bain groups. Therefore, the fraction of boundaries between different Bain groups is increased. Since the boundary between the variants with different Bain groups is the high angle, the multi-step austempering treatment increases the fraction of boundaries with large misorientation. This is demonstrated in Fig. 10 in which it is obvious that step austempering increased the fraction of the high-misorientation angle boundaries.

4. Conclusion

Multi-step austempering heat treatment was carried out to achieve ultra-fine bainitic microstructure and the desired mechanical characteristics of bainitic steel with 0.26 wt% carbon. The heat treatment process was conducted with partial bainitic transformation at the temperatures considerably lower than the M_S temperature of the steel. The results showed that the yield strength and impact fracture toughness of the steel were significantly improved by multi-step austempering treatment. The significant decrease in the volume fraction and size of the austenite/martensite blocks in the microstructure and the formation of nanoscale bainitic plates and austenitic films were the dominant factors in increasing the mechanical properties. It was also shown that the reduced austempering temperature in the second step decreased the thickness of the plates in the Bain groups; this change in the crystallographic characteristic led to an increase in the fraction of high angle boundaries in the microstructure, which played a significant role in increasing the impact fracture toughness of the steel.

Acknowledgements

Authors acknowledge Sahand University of Technology for providing the research facilities. AC and YTP thank for the financial support from the Faculty of Science and Engineering, University of Groningen, The Netherlands.

References

[1] F. Caballero, H. Bhadeshia, K. Mawella, D. Jones, P. Brown, Very strong low temperature bainite, Mater. Sci. Technol. 18 (3) (2002) 279–284.
[2] F. Caballero, H. Bhadeshia, Very strong bainite, Curr. Opin. Solid State Mater. Sci. 8 (3–4) (2004) 251–257.
[3] H. Bhadeshia, Bainite in Steels: Transformation, Microstructure and Properties, The Institute of Materials, University of Cambridge, London, 2001, pp. 377–382.
[4] T. Yokota, C.G. Mateo, H. Bhadeshia, Formation of nanostructured steels by phase transformation, Scr. Mater. 51 (8) (2004) 767–770.
[5] M. Yoozbashi, S. Yazdani, T. Wang, Design of a new nanostructured, high-Si bainitic steel with lower cost production, Mater. Des. 32 (6) (2011) 3248–3253.
[6] C. Garcia-Mateo, F. Caballero, H. Bhadeshia, Low temperature bainite, J. Phys. IV (Proc.) EDP Sci. (2003) 285–288.
[7] C. Garcia-Mateo, H. Bhadeshia, Acceleration of low-temperature bainite, ISIJ Int. 43 (11) (2003) 1821–1825.
[8] C. Garcia-Mateo, F.G. Caballero, H.K. Bhadeshia, Mechanical properties of low-temperature bainite, Mater. Sci. Forum Trans. Tech. Publ. (2005) 495–502.
[9] C. García-Mateo, F.G. Caballero, The role of retained austenite on tensile properties of steels with bainitic microstructures, Mater. Trans. 46 (8) (2005) 1839–1846.
[10] F.G. Caballero, C. GarcíA-Mateo, J. Chao, M.J. Santofimia, C. Capdevila, C.G. De Andres, Effects of morphology and stability of retained austenite on the ductility of TRIP-aided bainitic steels, ISIJ Int. 48 (9) (2008) 1256–1262.
[11] C. Garcia-Mateo, F. Caballero, J. Chao, C. Capdevila, C.G. De Andres, Mechanical stability of retained austenite during plastic deformation of super high strength carbide free bainitic steels, J. Mater. Sci. 44 (17) (2009) 4617–4624.
[12] B. Sandvik, H. Nevalainen, Structu re-property relationships in commercial low-alloy bainitic-austenitic steel with high strength, ductility, and toughness, Met. Technol. 8 (1) (1981) 213–220.
[13] G. Langford, M. Cohen, Calculation of cell-size strengthening of wire-drawn iron, Metall. Mater. Trans. B 1 (5) (1970) 1478–1480.
[14] C. Garcia-Mateo, H. Bhadeshia, Development of hard bainite, ISIJ Int. 43 (8) (2003) 1238–1243.
[15] H. Bhadeshia, Bainitic bulk-nanocrystalline steel, in: Proceedings of the 3rd International Conference on Advanced Structural Steels, 2006.
[16] H.S. Yang, J.H. Park, H. Bhadeshia, Possibility of Low-Carbon, Low-Temperature Bainite, International Conference on Martensitic Transformations (ICOMAT), Wiley Online Library, pp. 695–702.
[17] H.S. Yang, H. Bhadeshia, Designing low carbon, low temperature bainite, Mater. Sci. Technol. 24 (3) (2008) 335–342.
[18] Y. Shen, L. Qiu, X. Sun, L. Zuo, P.K. Liaw, D. Raabe, Effects of retained austenite volume fraction, morphology, and carbon content on strength and ductility of nanostructured TRIP-assisted steels, Mater. Sci. Eng.: A 636 (2015) 551–564.
[19] X. Long, F. Zhang, J. Kang, B. Lv, X. Shi, Low-temperature bainite in low-carbon steel, Mater. Sci. Eng.: A 594 (2014) 344–351.

[20] B. Avishan, M. Tavakolian, S. Yazdani, Two-step austempering of high performance steel with nanoscale microstructure, Mater. Sci. Eng.: A 693 (2017) 178–185.
[21] M. Soliman, H. Mostafa, A.S. El-Sabbagh, H. Palkowski, Low temperature bainite in steel with 0.26 wt% C, Mater. Sci. Eng.: A 527 (29–30) (2010) 7706–7713.
[22] X. Wang, K. Wu, F. Hu, L. Yu, X. Wan, Multi-step isothermal bainitic transformation in medium-carbon steel, Scr. Mater. 74 (2014) 56–59.
[23] Y.Y. Song, K.-S. Park, H. Bhadeshia, D.-W. Suh, Austenite in transformation-induced plasticity steel subjected to multiple isothermal heat treatments, Metall. Mater. Trans. A 45 (10) (2014) 4201–4209.
[24] K.-W. Kim, K.I. Kim, C.-H. Lee, J.-Y. Kang, T.-H. Lee, K.-M. Cho, K.H. Oh, Control of retained austenite morphology through double bainitic transformation, Mater. Sci. Eng.: A 673 (2016) 557–561.
[25] H.K.D.H. Bhadeshia, Materials algorithms project, Materials Algorithms Project ⟨https://www.msm.cam.ac.uk/map/steel/programs/mucg83.html⟩.
[26] Y.-W. Dong, Z.-H. Jiang, Z.-B. Li, Mathematical model for electroslag remelting process, J. Iron Steel Res. Int. 14 (5) (2007) 7–30.
[27] E. Kozeschnik, H. Bhadeshia, Influence of silicon on cementite precipitation in steels, Mater. Sci. Technol. 24 (3) (2008) 343–347.
[28] L. Chang, H. Bhadeshia, Austenite films in bainitic microstructures, Mater. Sci. Technol. 11 (9) (1995) 874–882.
[29] S.R.S.B.D. Cullity, Elements of X-Ray Diffraction, 3rd ed., Prentice Hall, New York, 2001.
[30] S. Singh, H. Bhadeshia, Estimation of bainite plate-thickness in low-alloy steels, Mater. Sci. Eng.: A 245 (1) (1998) 72–79.
[31] H. Bhadeshia, Nanostructured bainite, Proc. R. Soc. Lond. A: Math. Phys. Eng. Sci. R. Soc. (2010) 3–18.
[32] B. Avishan, C. Garcia-Mateo, L. Morales-Rivas, S. Yazdani, F.G. Caballero, Strengthening and mechanical stability mechanisms in nanostructured bainite, J. Mater. Sci. 48 (18) (2013) 6121–6132.
[33] B. Avishan, S. Yazdani, S.H. Nedjad, Toughness variations in nanostructured bainitic steels, Mater. Sci. Eng.: A 548 (2012) 106–111.
[34] A. Lambert-Perlade, A.F. Gourgues, J. Besson, T. Sturel, A. Pineau, Mechanisms and modeling of cleavage fracture in simulated heat-affected zone microstructures of a high-strength low alloy steel, Metall. Mater. Trans. A 35 (13) (2004) 1039–1053.
[35] S. Morito, H. Tanaka, R. Konishi, T. Furuhara, Maki, The morphology and crystallography of lath martensite in Fe-C alloys, Acta Mater. 51 (6) (2003) 1789–1799.
[36] S. Kang, J.G. Speer, R.W. Regier, H. Nako, S.C. Kennett, K.O. Findley, The analysis of bainitic ferrite microstructure in microalloyed plate steels through quantitative characterization of intervariant boundaries, Mater. Sci. Eng.: A 669 (2016) 459–468.